

ELECTRONIC AND OPTICAL PROPERTIES OF SEMICONDUCTORS

Charge Carrier Mobility in n - $\text{Cd}_x\text{Hg}_{1-x}\text{Te}$ Crystals Subjected to Dynamic Ultrasonic Stressing

A. I. Vlasenko, Ya. M. Olikh, and R. K. Savkina*

Institute of Semiconductor Physics, National Academy of Sciences of Ukraine, Kiev, 252028 Ukraine

* e-mail: savkina@class.semicond.kiev.ua

Submitted December 9, 1999; accepted for publication December 23, 1999

Abstract—The Hall mobility was studied in the n - $\text{Cd}_x\text{Hg}_{1-x}\text{Te}$ crystals subjected to dynamic ultrasonic stressing ($W_{US} \leq 10^4 \text{ W/m}^2$, $f = 5\text{--}7 \text{ MHz}$). It was found that, in field of the ultrasonic deformation, an increase in the carrier mobility in the impurity conduction region ($T < 120 \text{ K}$) and a decrease in the intrinsic conduction region ($T > 120 \text{ K}$) occurred in all tested samples. In this case, the magnitude of the sonic-stimulated variation in μ_H increases with decreasing structural perfection of a crystal. Different mechanisms of ultrasonic influence on μ_H with regard to scattering by optical phonons, ionized impurities, and alloy potential are analyzed, with the current flow conditions in the crystal taken into account. It is shown that, in the impurity conduction region, the main cause of the sonic-stimulated increase of the Hall mobility is the smoothing of the macroscopic intracrystalline potential that results from the inhomogeneity of the crystals. In the intrinsic conduction region, a decrease in mobility is caused by an increase in the intensity of scattering by the optical phonons. © 2000 MAIK “Nauka/Interperiodica”.

1. INTRODUCTION

Previously, it was found that transport coefficients of the $\text{Cd}_x\text{Hg}_{1-x}\text{Te}$ crystals are sensitive to the effect of the intense high-frequency alternating deformation, that is, to the ultrasonic effect both in the mode of ultrasound treatment [1, 2] and in the course of dynamic stressing [3–5]. Different mechanisms of acoustically stimulated irreversible variations of the electrical parameters (concentration and mobility) of the $\text{Cd}_x\text{Hg}_{1-x}\text{Te}$ crystals, including thermoacoustic annealing [1], destruction of the defect clusters [2], and so on, have been proposed. Processes of the ultrasound-induced transformation of the crystal defects in $\text{Cd}_x\text{Hg}_{1-x}\text{Te}$ were studied in [4, 5]. In this paper, we analyze mechanisms of the carrier mobility variations in the n - $\text{Cd}_x\text{Hg}_{1-x}\text{Te}$ crystals that have different degrees of structural perfection and are subjected to dynamic ultrasonic stressing.

2. EXPERIMENTAL RESULTS

Temperature dependences of the Hall mobility $\mu_H(T)$ in the n - $\text{Cd}_x\text{Hg}_{1-x}\text{Te}$ crystals ($0.2 \leq x \leq 0.22$ and $3 \times 10^{14} \text{ cm}^{-3} < n < 10^{15} \text{ cm}^{-3}$) in the intense field of the ultrasound-induced deformation ($W_{US} \leq 10^4 \text{ W/m}^2$, $f = 5\text{--}7 \text{ MHz}$) in the temperature range $T = 77\text{--}300 \text{ K}$ were studied. The experimental technique was described in [5].

Experimental curves of $\mu_H(T)$ for several samples with different μ_H^0 values at $T = 77 \text{ K}$ are shown in Fig. 1 (curves 1–4). The initial $\mu_H^0(T)$ dependences in the

intrinsic conduction region ($T > 120 \text{ K}$) are similar to the corresponding dependence in the structurally perfect crystals (dashed line), but, in the impurity conduction region, the mobility is lower. For samples 3 and 4, the slope of the $\mu_H^0(T)$ curve inverts at $T < 120 \text{ K}$ and the mobility has anomalously low values. This can be explained by the variation of the scattering mechanism that is observed in the $\text{Cd}_x\text{Hg}_{1-x}\text{Te}$ crystals at lower temperatures ($T < 50 \text{ K}$) [6, 7]. Apparently, these trends in $\mu_H(T)$ are related to the variation of the current flow conditions due to the bulk inhomogeneity of the crystals, which is confirmed by the form of the resistivity dependences on the magnetic field. In high magnetic fields ($B \geq 0.2 \text{ T}$), the resistivity does not saturate and magnetoresistance $\Delta\rho_{\perp}/\rho_0(B)$ increases linearly with B . It should be noted that, in sample 1, the magnetoresistance dependence on B is weak and the $\mu_H(T)$ dependence is the most similar to the mobility behavior in the structurally perfect crystal. In addition, in sample 4, the Hall coefficient R_H strongly depends on B ($>20\%$ for $B \leq 0.55 \text{ T}$). Apparently, at lower temperatures ($<77 \text{ K}$), conduction in the sample becomes of the p -type.

Under ultrasound stressing, an increase in $\mu_H^{US}/\mu_H^0 = 1.1\text{--}1.8$ in the impurity conduction region ($T < 120 \text{ K}$) and a decrease in the Hall mobility $\mu_H^{US}/\mu_H^0 = 0.83\text{--}0.93$ in the intrinsic conduction region are observed in all investigated samples (Fig. 1, curves 1'–4'). In this case, the magnetoresistance dependences $\Delta\rho_{\perp}/\rho_0(B)$ are saturated in high magnetic fields. Henceforth, the index US indicates that the parameter is mea-

sured in the field of the ultrasound-induced deformation, and the index 0 corresponds to the measurements in the absence of ultrasonic stressing (except for ρ_0 , which is the resistivity at $B = 0$). It should be noted that all observed acoustically stimulated variations have a reversible character. After switching off the ultrasound, mobility in the impurity conduction region returns to the initial values in the same time as the carrier concentration $(eR_H)^{-1}$. The conditions of our experiment do not allow us to say the same about mobility in the intrinsic conduction region.

The Raman spectra are shown in Fig. 2 for samples 3 and 4 with the largest influence of ultrasound on mobility. Curves 1' and 2' correspond to the ultrasonic stressing at room temperature. Curves 1 and 2 correspond to the measurements at the same temperature with an absence of ultrasonic stressing. The caption to Fig. 2 describes the conditions under which the spectra were measured.

The mobility dependences on the intensity of the ultrasonic stressing $\mu_H(\sigma_{US})$ at different temperatures are shown in Fig. 3. It can be seen that the form of the amplitude dependences $\mu_H(\sigma_{US})$ is governed by temperature. At $T = 83$ K (curve 1), μ_H increases linearly under the influence of the ultrasonic vibrations. At higher temperatures ($T = 93$ K, curve 2 and $T = 103$ K, curve 3), the mobility μ_H levels off after a small linear increase. As the temperature is further increased, an acoustically stimulated decrease in $\mu_H(\sigma_{US})$ ($T = 125$ K, curve 4) is observed.

3. DISCUSSION

Analyzing the experimental data, it should be noted that the acoustically stimulated variation of the Hall mobility can be related, first of all, to the variation in the conditions of charge-carrier scattering in the crystal in the presence of ultrasonic stressing. Another possible reason is the changing of the current flow conditions in an inhomogeneous crystal. Let us analyze these possible reasons in detail.

As has been established previously, for proper analysis of the $\mu_H(T)$ dependence in $\text{Cd}_x\text{Hg}_{1-x}\text{Te}$ at $T = 4$ –300 K, it is sufficient to consider three scattering mechanisms: by polar optical phonons (μ_{op}), by alloy potential (μ_{al}), and by ionized impurities (μ_{ion}) [8]. Such mechanisms as acoustic phonon scattering and electron–electron scattering do not provide a noticeable contribution to the total scattering process. Let us assume that, in the presence of ultrasonic stressing, the carrier scattering is determined by the same mechanisms:

$$\begin{aligned} (\mu_H^{US})^{-1} &= (e/m^*)^{-1} \sum (\tau_i^{US})^{-1} \\ &= (\mu_{op}^{US})^{-1} + (\mu_{al}^{US})^{-1} + (\mu_{ion}^{US})^{-1}. \end{aligned} \quad (1)$$

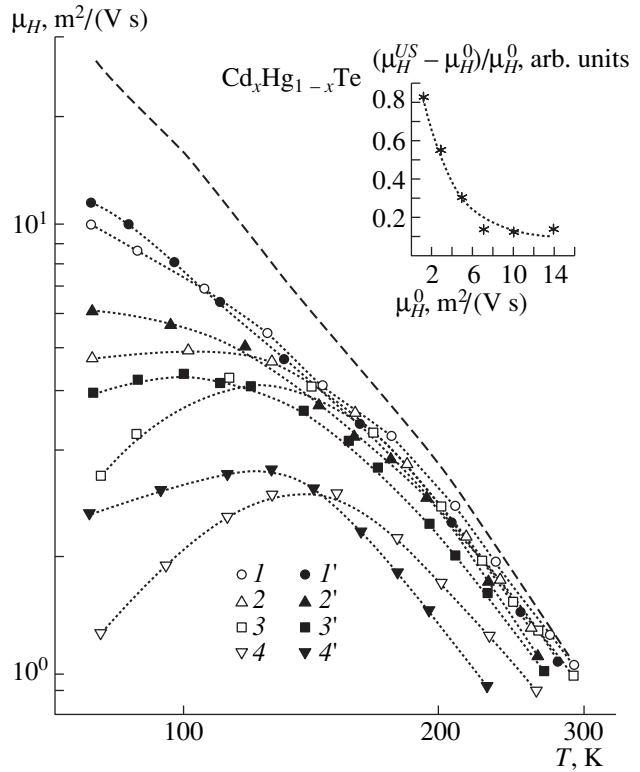


Fig. 1. Temperature dependences of the Hall mobility μ_H in the $\text{Cd}_x\text{Hg}_{1-x}\text{Te}$ crystals. Curves 1, 2, 3, and 4 were measured in the absence of ultrasound stressing, and curves 1', 2', 3', and 4' correspond to the samples subjected to ultrasound stressing ($\sigma_{US} = 4.8 \times 10^5$ Pa, $f = 6.5$ MHz). The $\mu_H(T)$ dependence for a structurally perfect crystal is given by the dashed line [6]. The dependence of the sonic-stimulated increase in the Hall mobility $\Delta\mu_{H,77}^{US} = (\mu_H^{US} - \mu_H^0)/\mu_H^0$ on the value of $\mu_{H,77}^0$ at $T = 77$ K and $\sigma_{US} = 4.8 \times 10^5$ Pa is shown in the insert.

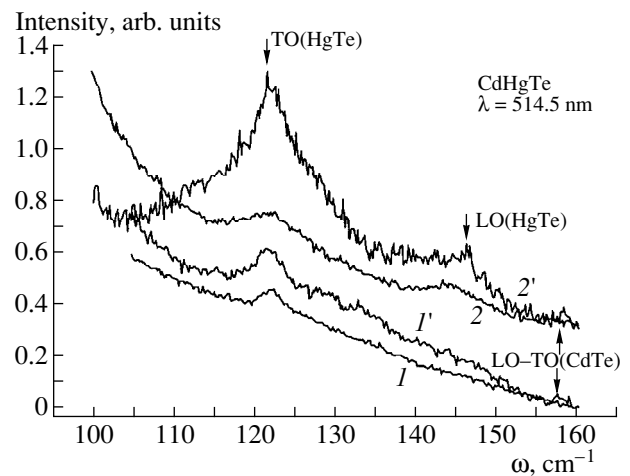


Fig. 2. Raman spectra of the $\text{Cd}_x\text{Hg}_{1-x}\text{Te}$ crystals (curves 1 and 1' correspond to sample 3; curves 2 and 2' correspond to sample 4). Curves 1' and 2' correspond to the sample subjected to ultrasound stressing, $T = 300$ K, $\sigma_{US} = 4.8 \times 10^5$ Pa.

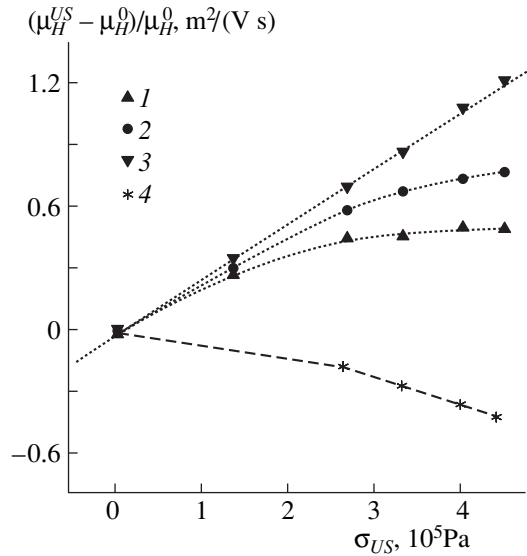


Fig. 3. Dependence of the carrier mobility on the amplitude of the ultrasound stressing of the $\text{Cd}_x\text{Hg}_{1-x}\text{Te}$ crystal (sample 3) at temperatures of (1) 83, (2) 93, (3) 103, and (4) 125 K.

Let us consider separately each of these mechanisms from the standpoint of its ultrasound-induced modification.

3.1. Ionized-Impurity Scattering

Ionized impurity scattering is dominant in $\text{Cd}_x\text{Hg}_{1-x}\text{Te}$ crystals at $T < 50$ K. Nevertheless, it is necessary to consider this mechanism at higher temperatures. The relaxation time for this mechanism can be given by [8]

$$\tau_{\text{ion}} = (\epsilon_s \hbar^3 / 2\pi e^4 N_i) (k^3 / m^*) (1/F_{\text{ion}}), \quad (2)$$

where F_{ion} is a function accounting for the symmetry of the electron wave functions and for the screening of the scattering center potentials by the free carriers, N_i is the concentration of the ionized impurities, $\epsilon_s = \epsilon_L + \epsilon_\infty$, ϵ_L is the dielectric constant of the CdTe and HgTe sublattices, and ϵ_∞ is the high-frequency dielectric constant. Other designations are as generally accepted.

It is well known that the essence of the processes that occur in $\text{Cd}_x\text{Hg}_{1-x}\text{Te}$ crystals under the influence of external factors, such as laser irradiation [9], deformation [10], γ -irradiation [11], ultrasonic treatment [1], etc., consists in the redistribution of the initial (native) defects or newly formed point defects between matrix and sinks (dislocations, small-angle boundaries, boundaries of subblocks, and so on). This process is governed by the initial state of the defects and causes variation of the material properties. One can assume that a similar situation takes place also in the case of dynamic below-threshold ultrasonic stressing of $\text{Cd}_x\text{Hg}_{1-x}\text{Te}$ crystals [4, 5]. In accordance with general

mechanisms of the defect transformation in $\text{Cd}_x\text{Hg}_{1-x}\text{Te}$ in the field of intense ultrasound-induced deformation, a temporary (during the ultrasound action) detachment of the point defects (for example, Hg or background-impurity atoms) from dislocations and small-angle boundaries to the interstices of matrix and (or) capture of vacancies by the linear defects are possible. In this case, the concentration of donors $N_d^0 + N_d^{US}$ should increase and the concentration of acceptors $N_a^0 - N_a^{US}$ should decrease. Therefore, in the presence of ultrasonic stressing, the concentration of the scattering centers N_i should be changed. Let us express N_i^{US} , without consideration of the ionization degree of the defects, as

$$N_i^{US} = N_i^0 + \Delta N_i = N_i^0 + (N_d^{US} - N_a^{US}). \quad (3)$$

At $T = 77$ K and $\sigma_{US} = 4.8 \times 10^5$ Pa, ultrasound-induced variation of carrier concentration from $n_0 = 7.5 \times 10^{14} \text{ cm}^{-3}$ to $n_{US} = 8.5 \times 10^{14} \text{ cm}^{-3}$ is observed for sample 1, from $n_0 = 3.2 \times 10^{14} \text{ cm}^{-3}$ to $n_{US} = 4 \times 10^{14} \text{ cm}^{-3}$ for sample 2, from $n_0 = 3 \times 10^{14} \text{ cm}^{-3}$ to $n_{US} = 6 \times 10^{14} \text{ cm}^{-3}$ for sample 3, and from $n_0 = 9 \times 10^{14} \text{ cm}^{-3}$ to $n_{US} = 1.5 \times 10^{15} \text{ cm}^{-3}$ for sample 4. Concentration variation $(n_{US} - n_0)$ corresponds to the ΔN_i value. In the tested samples, N_i^0 does not exceed $5 \times 10^{15} \text{ cm}^{-3}$. Taking into account (3), we easily derive the relation between μ_{ion}^0 and μ_{ion}^{US} as

$$(\mu_{\text{ion}}^{-1})^{US} = (\mu_{\text{ion}}^{-1})^0 (1 + \Delta N_i / N_i^0), \quad (4)$$

from which, considering the aforementioned estimates of ΔN_i and N_i^0 , we obtain the ratio $\mu_{\text{ion}}^{US} / \mu_{\text{ion}}^0 = (0.99 - 0.89)$. This shows that the intensity of scattering by the ionized impurities increases due to an acoustically stimulated increase in the concentration of scattering centers. Therefore, this mechanism does not allow us to explain an increase in the mobility μ_H , which is observed in the experiment.

As one can see from (2), another cause of mobility variation in the case of scattering by the ionized impurities may be an increase in the free carrier concentration n in the crystal. This results, first, in more effective screening of the Coulomb potential of scattering centers, and, therefore, in a decrease in the contribution of this mechanism to the total scattering. This assumption is confirmed by calculations of the $F_{\text{ion}}(n)$ dependence: an increase in n from 10^{14} to 10^{15} cm^{-3} leads to $F_{\text{ion}}^{US} / F_{\text{ion}}^0 = 0.95$ and, as a result, to an insignificant increase in the mobility ratio $\mu_{\text{ion}}^{US} / \mu_{\text{ion}}^0 = 1.05$. Furthermore, an increase in the carrier concentration causes also an increase in mobility μ_{ion} due to an increase in the average electron energy [12]. However, although

this mechanism results in an increase in mobility, it does not enable us to explain quantitatively the experimental results for all tested samples, in particular, for the dependence of the ultrasound-induced mobility increase on the $\mu_{H,77}^0$ value measured in the absence of the ultrasonic deformation. Dependence of the acoustically stimulated increase in the Hall mobility $\Delta\mu_{H,77}^{US}$ on the $\mu_{H,77}^0$ value is presented in Fig. 1 (see the inset). The larger the value of $\mu_{H,77}^0$, the less pronounced the ultrasound effect (that is, $\Delta\mu_{H,77}^{US}$) for equal values of the intensity of the ultrasound stressing.

3.2. Scattering by the Alloy Potential

Scattering by the alloy potential arises from the disturbance in periodicity of the crystal potential in $A_xB_{1-x}C$ solid solutions due to disorder in the arrangement of the A and B atoms in the sites of the crystal lattice. Study of this mechanism is based on the assumption that the difference between the A and B atomic potentials $U_{AB}(r) = U_A - U_B$ is a small perturbation. In addition, the U_{AB} potential is localized: $U_{AB} = \Delta E$ for $r < r_0$ and $U_{AB} = 0$ for $r > r_0$, where r_0 is the distance between the nearest neighbors [13].

The relaxation time for alloy scattering may be expressed as [14]

$$\tau_{al} = (\pi N_0 / \hbar x(1-x)\Delta E^2)(k^{-3}(d\varepsilon/dk)^2), \quad (5)$$

where ΔE is the alloy scattering potential, N_0 is the number of atoms in the unit volume, and x is the composition parameter. The value of ΔE is assumed, in the first approximation, to be equal to the difference between the band gaps of the AC and BC crystals [15, 16]. It is proposed in [14] to choose ΔE as the difference between the A and B atomic screened potentials. In this case, the value of the alloy potential for $Cd_xHg_{1-x}Te$ is $\Omega\Delta E = 9 \times 10^{-29}$ eV cm³, $\Delta E = 1$ eV [14, 17] and Ω is the volume of the unit cell. A much smaller value $\Delta E = 0.23$ eV obtained from calculations in the coherent potential approximation [18] was successfully used in [19] in calculations of the mobility temperature dependences. It should be noted that, most often, ΔE is used as an adjustable parameter determined from a comparison of the calculated and experimental data.

As in the above case of the ionized impurity scattering, it is possible to assume the existence of several mechanisms of the ultrasound-induced modification of scattering by the disorder of the crystal lattice. First, due to the μ_{al} dependence on the electron energy ($\sim \varepsilon^{-1/2}$) [14], an acoustically stimulated increase in the carrier concentration should enhance scattering by the alloy potential. Calculations at $T = 10$ K show that the contribution of this mechanism increases from 5% for $n = 4 \times 10^{14}$ cm⁻³ to 25% for $n = 2 \times 10^{16}$ cm⁻³ [20].

A similar result was obtained in [12] at $T = 77$ K. Thus, due to the acoustically stimulated increase of n , the mobility limited by the alloy scattering should decrease, which excludes this mechanism from consideration, because it does not correspond to the experimentally observed effect.

The deformation mechanism of the ultrasound influence on the alloy potential is quite possible if we choose the latter as the difference between the CdTe and HgTe band gaps. However, calculations show that, at the intensities of ultrasound-stressing used in the experiment, the value of the effective pressure P generated by the ultrasonic wave in crystal does not exceed 5×10^5 Pa. In this case, the alloy potential in the field of the ultrasound-induced deformation $\Delta E^{US} = [\varepsilon_g^0 + (d\varepsilon_g/dP)P]_{CdTe} - [\varepsilon_g^0 + (d\varepsilon_g/dP)P]_{HgTe}$ decreases by a negligible value (no more than $\sim 5 \times 10^{-5}$ eV). Finally, since the carrier concentration increases in the ultrasound field, it is possible to assume that the alloy potential has additional screening. However, in the case of alloy scattering, it is not clear if screening significantly changes the localized potential ΔE [14].

Thus, the analysis shows that it is impossible to explain the effect of the ultrasound-induced increase of the Hall mobility in the impurity conduction region only on the basis of variation of the scattering conditions.

3.3. Ultrasound-Stimulated Modification of the Large-Scale Crystal Potential

Another possible cause of the acoustically stimulated increase in mobility μ_H is variation of the current flow conditions in the sample due to the ultrasound-induced modification of the intracrystalline potential. We have in mind the large-scale potential, whose specific dimension exceeds the carrier free path, and, therefore, we do not consider the influence of this potential on the electron scattering processes. It is well known that reduced (in comparison with the theoretical values) carrier mobilities and the anomalous decrease of $\mu_H(T)$ in the impurity conduction region at $T < 120$ K, which we observed in the tested samples, cannot be explained by additional scattering mechanisms. This shows that there are drift barriers in the crystal related to the covariant and contravariant modulation of the crystal energy bands in the inhomogeneous samples [21, 22]. At the same time, the larger the size of inhomogeneity, the greater the difference between the Hall mobility and the drift mobility. The presence of the bulk inhomogeneities in the samples is confirmed, as we mentioned above, by the linear dependence of $\Delta\rho_{\perp}/\rho_0(B)$ in the high magnetic fields.

In our opinion, the intracrystalline potential is smoothed in the field of the ultrasound-induced deformation. The point defects localized at (or near) the extended defects absorbing the ultrasound wave are

transferred to the matrix under the effect of the acoustic field and cause the hillocks in the potential relief to flatten. In this case, a larger crystal volume is involved in conduction at the percolation level. The increase of the Hall mobility in the impurity conduction region ($T < 120$ K) and the saturation of the magnetoresistance $\Delta\rho_{\perp}/\rho_0(B)$ in the high magnetic fields in the samples subjected to ultrasonic stressing confirm these assumptions.

It is necessary to make clear that, by inhomogeneities, which give rise to the large-scale potential, we mean dislocations with the surrounding impurities, the dislocation clusters, the low-angle boundaries, inclusions of the second phase of the basic components of the solid solution, impurities which appear near dislocations, and other defects. Considering the sonic-dislocation mechanism as dominant in the ultrasound-wave interaction with crystal and absorption of the ultrasonic energy near such macrodefects, we can also assume that smoothing of the large-scale potential is governed by the ultrasound-initiated deionization of the levels localized at the dislocation line. In the initial state, these levels capture the majority carriers and form impermeable inclusions. The acoustically stimulated increase in the electron concentration in the impurity conduction region supports this assumption [5]. However, study of the relaxation time of the acoustically stimulated processes in n -CdHgTe show that, after relief of the ultrasound stressing, concentration and mobility return to the initial values in $\sim 10^2$ – 10^3 s. This suggests that the ultrasound-stimulated transformations involve diffusion rather than recombination, because, in the latter case, the typical relaxation time is $\sim 10^{-6}$ – 10^{-7} s.

It should be also noted that, in spite of the key role of dislocations in the ultrasonic effects in the CdHgTe crystals, we do not consider scattering by dislocations, because the contribution of this mechanism becomes appreciable at temperatures < 50 K for a dislocation density of $N_d > 10^6$ cm $^{-2}$ [23]. However, in the investigated samples, N_d does not exceed 10^5 cm $^{-2}$. In addition, we do not exclude the possibility of the ultrasound-induced formation, under certain conditions, of a parallel conduction channel with carrier mobility higher than that in the matrix. However, further studies are needed to confirm this conclusion.

3.4. Optical Phonon Scattering

We now attempt to explain the decrease of the carrier mobility in the intrinsic conduction region. It has been established that scattering by the optical phonons is dominant in the CdHgTe crystals in the temperature range of 77–300 K. Therefore, a decrease in the carrier mobility in the field of the ultrasound-induced deformation in the intrinsic conduction region, which we observed in all tested samples, can be explained by the ultrasound-induced modification of the CdHgTe

phonon spectrum. Actually, in the field of the ultrasound-induced deformation, an increase in the band intensity of the Raman spectra occurs (Fig. 2). We may relate this result to an increase in the crystal's effective temperature, which causes the rate of scattering by optical phonons to increase. Attention is attracted to the fact that the ultrasound influence on the Raman spectra correlates with the magnitude of the acoustically stimulated variation of mobility in these samples. Further studies are necessary for quantitative estimations. We only note that, both in the impurity conduction and intrinsic conduction regions, an increase in the rate of scattering by optical phonons also occurs.

The competition of the scattering processes mentioned above gives an adequate explanation of the Hall mobility dependences on the intensity of the ultrasound stressing $\mu_H(\sigma_{US})$ at different temperatures (Fig. 3). At lower temperatures, the form of the $\mu_H(\sigma_{US})$ dependence is determined by the acoustically induced smoothing of the intracrystalline potential, i.e., by variation of the current flow conditions under ultrasound stressing due to an increase in the effective crystal volume at the percolation level. As temperature increases, the concentration distribution over the crystal becomes uniform and the space-charge regions disappear. In this case, the contribution of the crystal lattice vibrations increases and the efficiency of this mechanism in the field of the ultrasound-induced deformation also increases. This accounts for the fact that the curve $\mu_H(\sigma_{US})$ first levels off and then descends. Now the dependence of the ultrasound-induced increase of μ_H on the value of $\mu_{H,77}^0$ becomes quite clear. The least pronounced effect is observed in sample 1, which has the most perfect structure and the highest value of $\mu_{H,77}^0$. It is reasonable to assume that, in the uniform CdHgTe crystal in which it is possible to neglect the influence of the large-scale potential, the ultrasound-induced decrease in the carrier mobility would occur in the temperature range of 77–300 K due to an increase in the rate of scattering by optical phonons and alloy potential.

CONCLUSION

Thus, we observed an increase in the Hall mobility in the impurity conduction region ($T < 120$ K) in Cd $_x$ Hg $_{1-x}$ Te crystals subjected to dynamic ultrasound stressing. The magnitude of the sonic-stimulated variation in μ_H increases with the decreasing structural perfection of a crystal. We also observed a mobility decrease in the intrinsic conduction region ($T > 120$ K) for all investigated samples. We analyzed the possible mechanisms of the ultrasound influence on the μ_H taking into account scattering by optical phonons, ionized impurities, alloy potential, and the conditions of the current flow in the crystal. In the impurity conduction region, the principal cause of the ultrasound-induced

increase in the Hall mobility is the smoothing of the macroscopic intracrystalline potential determined by the inhomogeneity of the tested crystals. In the intrinsic conduction region, a decrease in mobility is attributed to an increase in the rate of scattering by optical phonons.

REFERENCES

1. K. A. Myslivets and Ya. M. Olikh, *Fiz. Tverd. Tela* (Leningrad) **32**, 2912 (1990) [*Sov. Phys. Solid State* **32**, 1692 (1990)].
2. P. I. Baranskiĭ, A. E. Belyaev, S. M. Komirenko, and N. V. Shevchenko, *Fiz. Tverd. Tela* (Leningrad) **32**, 2159 (1990) [*Sov. Phys. Solid State* **32**, 1257 (1990)].
3. A. V. Lyubchenko and Ya. M. Olikh, *Fiz. Tverd. Tela* (Leningrad) **37**, 2505 (1985) [*Sov. Phys. Solid State* **27**, 1500 (1985)].
4. O. I. Vlasenko, Ya. M. Olikh, and R. K. Savkina, *Ukr. Fiz. Zh.* **44**, 618 (1999).
5. A. I. Vlasenko, Ya. M. Olikh, and R. K. Savkina, *Fiz. Tekh. Poluprovodn. (St. Petersburg)* **33**, 410 (1999) [*Semiconductors* **33**, 398 (1999)].
6. A. I. Vlasenko, A. V. Lyubchenko, and E. A. Sal'kov, *Ukr. Fiz. Zh.* **25**, 1318 (1980).
7. Y. Y. Dubowski, T. Dietl, W. Szymanska, and R. R. Galaska, *J. Phys. Chem. Solids* **42**, 351 (1981).
8. W. Szymanska and T. Dietl, *J. Phys. Chem. Solids* **39**, 1025 (1978).
9. A. I. Vlasenko, K. R. Kurbanov, A. V. Lyubchenko, and E. A. Sal'kov, *Ukr. Fiz. Zh.* **25**, 1392 (1980).
10. S. G. Gasan-zade, *Optoelektron. Poluprovodn. Tekh.* **33**, 91 (1998).
11. A. I. Vlasenko, V. V. Gorbunov, and A. V. Lyubchenko, *Ukr. Fiz. Zh.* **29**, 423 (1984).
12. I. R. Gorokhovskii, A. K. Laurinavichyus, Yu. K. Pozhela, *et al.*, *Fiz. Tekh. Poluprovodn. (Leningrad)* **21**, 1998 (1987) [*Sov. Phys. Semicond.* **21**, 1211 (1987)].
13. P. N. Gorleĭ and V. A. Shenderovskii, *Variational Methods in the Kinetic Theory* (Naukova Dumka, Kiev, 1992).
14. J. Kossut, *Phys. Status Solidi B* **86**, 593 (1978).
15. D. Chattopadhyay and B. R. Nag, *Phys. Rev. B* **12**, 5676 (1975).
16. L. Makowski and M. Glicksman, *J. Phys. Chem. Solids* **34**, 487 (1973).
17. Y. Y. Dobowski, *Phys. Status Solidi B* **85**, 663 (1978).
18. K. C. Hass, H. Ehrenreich, and B. Velicky, *Phys. Rev. B* **27**, 1088 (1983).
19. P. Moravec, R. Grill, J. Franc, *et al.*, *Proc. SPIE* **3890**, 307 (1999).
20. F. J. Bartoli, C. A. Hoffman, and J. R. Meyer, *J. Vac. Sci. Technol. A* **1**, 1669 (1983).
21. M. A. Kinch, M. J. Brau, and A. Simmons, *J. Appl. Phys.* **44**, 1649 (1973).
22. M. K. Sheĭnkman and A. Ya. Shik, *Fiz. Tekh. Poluprovodn. (Leningrad)* **10**, 209 (1976) [*Sov. Phys. Semicond.* **10**, 128 (1976)].
23. H. Oszwaldowski, *J. Phys. Chem. Solids* **46**, 791 (1985).

Translated by I. Kucherenko